

Single-molecule fluorescence near a metal layer

Jörg Enderlein *

Institute of Analytical Chemistry, Chemo- and Biosensors, University of Regensburg, PF 10 10 42, D-93040 Regensburg, Germany

Received 15 December 1998

Abstract

A theoretical study of the fluorescence emission properties of a single dye molecule near a metal film is presented. The study accounts not only for the well-known fluorescing quenching of a dye near a metal interface, but also for the reduced photobleaching rate due to the enhanced de-excitation rate. It is shown that despite the high fluorescence quenching rates, the increased photostability of the molecule makes spectroscopic studies on single-molecule level feasible. © 1999 Elsevier Science B.V. All rights reserved.

1. Introduction

The fluorescence of single molecules is a fascinating research topic. The fluorescence emission of almost all molecules can be described fairly well by an electric-dipole model. Thus, studying the fluorescence characteristics (mainly angular distribution, polarization and lifetime) of a single molecule is equivalent to studying the electrostatics of a single, nearly point size dipole (from an optical point of view). Apart from the emission of such a dipole within a dielectrically homogeneous environment (free-dipole emission), the interaction of an emitting dipole with dielectric or metallic interfaces or cavities offers a rich playground for studying basic questions in electrostatics, and also for obtaining valuable insight into the details of the fluorescing molecule's photophysics.

In a series of seminal papers, Drexhage et al. studied the interaction of a layer of fluorescing dye

(europium chelates) with a metal interface already in the 1960s (see review [1]). In these papers, the main question was the dependence of the emission rate (viz. fluorescence lifetime) on the distance between the dye layer and the metal surface. The ultimate theoretical description of these experiments was presented in an excellent paper by Chance et al. [2].

In another series of theoretical papers, Lukosz and Kunz [3–8] studied in detail the interaction of fluorophores with dielectric interfaces and layers. Inspired by this theoretical work, Lieberherr et al. [9,10] performed a number of experiments concerned with the emission of fluorescent dyes within solvents with different dielectric constants, and of dye layers adsorbed on substrates with different dielectric constants. The main goal of these experiments was, by changing the dielectric properties of the dye environment and thus influencing only the radiative transition rate of the excited molecule, to obtain direct information about the radiative and non-radiative transition rates of the studied dye molecules. All these experiments were always performed on large ensembles of molecules.

* Tel.: +49-941-943-4048; fax: +49-941-943-4491; e-mail: joerg.enderlein@chemie.uni-regensburg.de

With the advent of single-molecule detection by laser-induced fluorescence, it became possible to study the emission of a single fluorophore and its interaction with interfaces or cavities. The big advantage of this single-molecule approach is that one can study fluctuations in the molecular behavior which are usually averaged out when performing measurements on large ensembles of molecules. The most striking example is the so-called blinking behavior of single fluorophores, when the molecule switches repeatedly between a fluorescing state and a non-fluorescing dark state [11–18].

By placing the molecules near interfaces with different dielectric properties (without changing anything else in their environment) and comparing their fluorescence behavior, one can gain deeper insight into the photophysical mechanisms governing their fluorescence, in analogy to the work of Lieberherr et al. concerning monomolecular dye layers. In this respect, changing the electromagnetic environment of a molecule by placing it at different distances from a metal film/surface is the most elegant way, because the distance between the molecule and the metal surface can be adjusted with great precision (by Langmuir–Blodgett films as spacer [1]), and when changing this distance, no other environmental property is changed. Thus, the system single molecule–dielectric–metal is an ideal system to study the electro-dynamics of fluorescence emission.

However, metal layers are of great importance also from a completely different point of view. Metal surfaces play a unique role in biomolecular activities such as the self-assembly and self-organization of proteins and lipids, a topic which has recently attracted a great deal of attention. In [19], Yokota et al. report the first successful detection of single tetramethylrhodamine and Cy5 molecules attached to protein molecules on metal surfaces.

One apparent difficulty with such an experimental approach is that for close distances (and thus strong interactions) between a fluorescing molecule and a metal surface, large fluorescence quenching effects should be expected, due to an increasing energy transfer from the excited molecule to the metal. Thus, one could expect to be unable to see a sufficiently large fluorescence signal from a single molecule to make such an experiment feasible. However, it is often overseen that the same energy trans-

fer that quenches the fluorescence also enhances the photostability of the molecule due to the shortening of the excited-state lifetime. This can be seen with the following simple rate argument: If the non-radiative decay rate is k_{nr} , if the radiative decay rate and yield are k_f and Q_f , and the photobleaching rate and yield are k_b and Q_b , then one has immediately that the number of emitted photons is $N = k_f/k_b = Q_f/Q_b$. In other words, the number of emitted photons does not depend on the non-radiative decay rate, k_{nr} . Already Hirschfeld [20] pointed out that, when dealing with single molecules, the fluorescence quantum-yield is not as important as the average number of fluorescence photons that are emitted by a molecule until photobleaching. Thus, when considering the feasibility of single molecule spectroscopy experiments near a metal surface, one has to study the overall number of detectable luminescence photons taking into account the fluorescence quenching, additional radiative decay channels, and the increased photostability, since the relevant parameter to single molecule experiments is the total number N of emitted photons; instead of computing the apparent quantum yield [1,2] we will compute N . In the present paper, we give a comprehensive theoretical study of this problem. In Section 2, a brief overview of the theoretical approach used is given. In Section 3, numerical results are presented for a realistic experimental configuration (single-molecule fluorescence at 670 nm near an aluminum film).

2. Theory

The theoretical framework of our study will be a semiclassical approach that is completely equivalent to a quantum-mechanical treatment which is based on electromagnetic-field mode density calculations [21]. The system studied is depicted in Fig. 1. In order to perform an experiment where a single molecule is positioned at different distances relative to the metal film, some sort of solid support is necessary. A molecule is adsorbed directly on a glass cover slip (refractive index n_{gl}) which is covered by a layer of thickness h of spacer molecules with refractive index n_w . On top of this layer, a metal film with complex refractive index n_m and thickness d is deposited. For simplicity, the half-space above

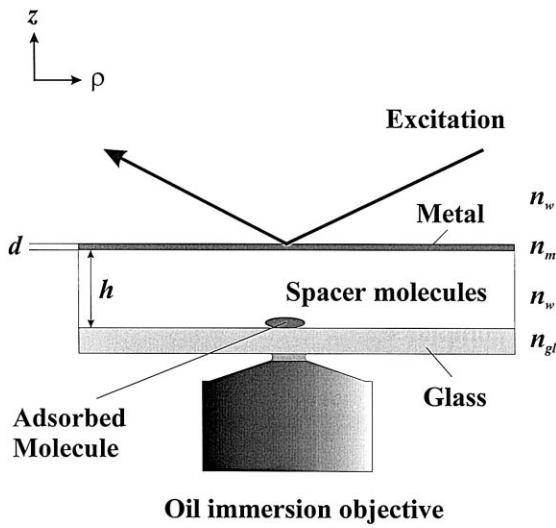


Fig. 1. Schematic view of the studied experimental set-up. A fluorescing dye molecule is adsorbed on a glass cover-slip with refractive index n_{gl} . On the cover slip, a layer of spacer molecules is deposited, e.g. by a Langmuir–Blodgett technique. This layer has a thickness h and a refractive index n_w . On top of this layer, a thin metal film with thickness d and refractive index n_m is sputtered. The refractive index of the medium above the metal film is the same as that of the spacer layer. Fluorescence excitation is assumed to be done by the evanescent field of a laser beam which is directed onto the metal film from above. Fluorescence detection is performed by an oil-immersion objective from below.

the metal layer is assumed to have the same refractive index n_w as the layer of spacer molecules. In a real experiment, the fluorescence excitation would preferably be done through the metal film in an evanescent manner (for reducing scattering and back-reflection of the exciting light), and the detection would be done through the cover slip with a high-numerical-aperture oil immersion objective. The question we will study here is how many photons will be, on average, detected from a single molecule, and the dependence of this number upon the metal film distance h and the film thickness d . To answer this question, we will calculate two quantities: the total emission rate of the emitting dipole, and the amount of light emitted into the light-collecting microscope objective.

The total emission rate can be found in the following way. First, one considers the electric field \vec{E}_D of an emitting free dipole embedded within a homogeneous medium with refractive index n_w . Second,

one determines the back-reaction field \vec{E}_R generated by the interaction of the free field with the glass and the metal film. This back-reaction field performs work on the dipole, which may enhance or suppress the dipole emission. The total emission rate S is then the sum of the emission rate of the free dipole, $S_0 = \omega n_w k_0^3 p^2 / 3$, plus a contribution caused by the back reaction of \vec{E}_R on the dipole, and is given by [2]:

$$S = \frac{\omega n_w k_0^3 p^2}{3} + \frac{\omega}{2} \vec{p} \cdot \text{Im} \vec{E}_R(0), \quad (1)$$

where \vec{p} is the dipole moment amplitude, k_0 is the vacuum wave vector amplitude of light, $k_0 = \omega/c$, ω is the oscillation frequency of the dipole, c is the vacuum speed of light, and $\vec{E}_R(0)$ is the back reaction field amplitude at the dipole's position.

Thus, one has to determine the value of the back reaction field at the dipole's position. We start with the following plane-wave integral representation of the electric field amplitude \vec{E}_D of the emission field of a fluorescing molecule (within a homogeneous medium with refractive index n_w), which is considered to be an ideal oscillating electric dipole:

$$\vec{E}_D(\vec{r}) = \frac{1}{n_w^2} \int \frac{d^3 \vec{k}}{2\pi^2} \left[k^2 \vec{p} - \vec{k}(\vec{k} \cdot \vec{p}) \right] \frac{\exp(i\vec{k} \cdot \vec{r})}{k_w^2 - k^2}. \quad (2)$$

Here, k_w is an abbreviation for the wave-vector amplitude $n_w \omega/c$; \vec{r} is the three-dimensional coordinate vector of the point where the electric field amplitude is calculated (the molecule's position is assumed to be the coordinate system's origin); \vec{k} is a three-dimensional integration variable, $\int d^3 \vec{k}$ symbolizes integration over the three-dimensional \vec{k} -space.

Performing in Eq. (2) the integration along the vertical direction (z -direction in Fig. 1), one arrives at

$$\vec{E}_D = \frac{i}{2\pi n_w^2} \int \frac{d^2 \vec{q}}{l_w} \left[k_w^2 \vec{p} - \vec{k}_w^\pm (\vec{k}_w^\pm \cdot \vec{p}) \right] \times \exp(i\vec{q} \cdot \vec{\rho} + il_w |z|), \quad (3)$$

where we used the abbreviations $\vec{r} = (\vec{\rho}, z)$, $\vec{k}_w^\pm = (\vec{q}, \pm l_w)$, $l_w = \sqrt{k_w^2 - q^2}$, $k_w^2 \equiv (k_w^\pm)^2$, and $\int d^2 \vec{q}$ denotes integration over the whole two-dimensional

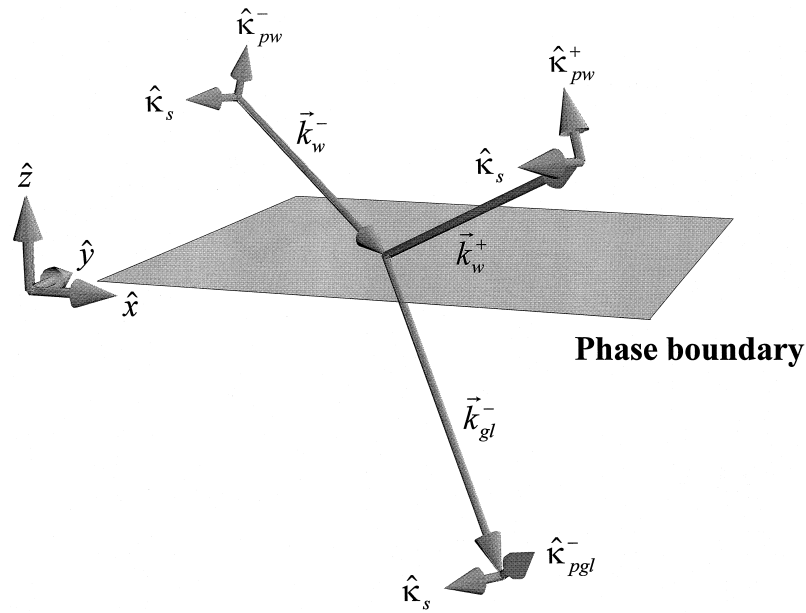


Fig. 2. Geometry of the plane-wave reflection and transmission at the spacer/glass boundary. A similar geometry applies for the spacer/metal boundary.

\vec{q} -space. The plus sign in the above equation applies if $z > 0$, the minus sign if $z < 0$. The vectors $\vec{\rho}$ and \vec{q} are the vector parts of \vec{r} and \vec{k}_w^\pm perpendicular to the z -direction. The value of l_w is assumed to lie always within the first quadrant of the complex plane. In deriving Eq. (3) by performing the integration in Eq. (2), Sommerfeld's radiation condition was taken into account (only outgoing plane waves can occur in Eq. (3)). The plane-wave representation of Eq. (3) is completely equivalent to the Hertz vector-approach as used in Ref. [2], Ch. 2. By rewriting the two-dimensional vector \vec{q} as $\vec{q} = u(\cos \psi, \sin \psi)$ and performing explicitly the integration over ψ in Eq. (3), one arrives at a similar integral representation for the electric field amplitude as presented in Ref. [2].

In the next step, it is useful to separate in Eq. (3) explicitly p -waves (magnetic field vector parallel to the interfaces) and s -waves (electric field vector parallel to the interfaces). By direct substitution, the following relation can be proved for $\vec{k}_w^\pm = (\vec{q}, \pm l_w)$:

$$\vec{k}_w^\pm \otimes \vec{k}_w^\pm - (k_w^\pm)^2 \hat{I} = (k_w^\pm)^2 (\hat{k}_{pw}^\pm \otimes \hat{k}_{pw}^\pm + \hat{k}_s \otimes \hat{k}_s) \quad (4)$$

where \hat{I} is the unit matrix, the symbol \otimes denotes tensorial multiplication, $(\vec{a} \otimes \vec{b})_{jk} = a_j b_k$, and the unit vectors \hat{k}_{pw}^\pm and \hat{k}_s are given by

$$\hat{k}_{pw}^\pm = \frac{1}{k_w} (\mp l_w \hat{q}, q) \quad (5)$$

$$\hat{k}_s = (\hat{z} \times \hat{q}, 0)$$

where \hat{q} and \hat{z} are unit vectors along \vec{q} and the z -axis, respectively (see Fig. 2). The unit vectors \hat{k}_{pw}^\pm and \hat{k}_s are the electric field polarization unit vectors of p - and s -waves with respect to the plane $z = 0$ (see Fig. 2). Substituting Eq. (4) into Eq. (3), one obtains

$$\vec{E}_D = \frac{ik_0^2}{2\pi} \int \frac{d^2\vec{q}}{l_w} \left[\hat{k}_{pw}^\pm (\hat{k}_{pw}^\pm \cdot \vec{p}) + \hat{k}_s (\hat{k}_s \cdot \vec{p}) \right] \times \exp(i\vec{q} \cdot \vec{\rho} + il_w |z|). \quad (6)$$

The last equation is the plane wave representation of the electric field of a free dipole embedded within a homogeneous medium with refractive index n_w . Interaction of this dipole field with the dielectric interfaces as depicted in Fig. 1 results in the back-reflection field \vec{E}_R . The simplest way to calculate this

field is by calculating the multiple reflections for all the plane waves in Eq. (6). For doing so, one has first to know the reflection coefficients for a single reflection of the p - and s -waves at the upper (spacer/metal) and lower (spacer/glass) interfaces. These coefficients are functions of the wave vector component l_w . For the lower interface, the (single) reflection coefficients are simply given by Fresnel's formulas ($(l_{gl} = \sqrt{n_{gl}^2 - n_w^2 + l_w^2})$) [22]:

$$r_p^0(l_w) = \frac{n_{gl}^2 l_w - n_w^2 l_{gl}}{n_{gl}^2 l_w + n_w^2 l_{gl}}, r_s^0(l_w) = \frac{l_w - l_{gl}}{l_w + l_{gl}}, \quad (7)$$

where r_p^0 refers to a p -wave reflection, and r_s^0 to a s -wave reflection, and the superscript 0 indicates that the coefficients refer to a reflection at the lower interface. The reflection coefficients at the metal layer can be derived by a transfer matrix approach and read in our case (with abbreviation $l_m = \sqrt{n_m^2 - n_w^2 + l_w^2}$):

$$r_p^1(l_w) = \frac{(e^{2idl_m} - 1)(l_w^2 n_m^4 - n_w^4 l_m^2)}{(e^{2idl_m} - 1)(l_w^2 n_m^4 + n_w^4 l_m^2) - 2(e^{2idl_m} + 1)n_m^2 n_w^2 l_m l_w},$$

$$r_s^1(l_w) = \frac{(e^{2idl_m} - 1)(l_w^2 - l_m^2)}{(e^{2idl_m} - 1)(l_w^2 + l_m^2) - 2(e^{2idl_m} + 1)l_m l_w}, \quad (8)$$

where, again, the subscripts denote the p - and s -wave reflection, and the superscript 1 indicates that the reflection takes place at the upper interface.

When calculating the field \vec{E}_R , one has to take into account all the infinite multiple reflections of the plane waves at the two interfaces. Four qualitatively different cases have to be distinguished: the plane wave is reflected an uneven number of times, with the first reflection either at the upper interface (Fig. 3a), or at the lower interface (Fig. 3b); alternatively the plane wave is reflected an even number of times, with the first reflection either at the upper interface (Fig. 3c), or at the lower interface (Fig. 3d). For our further purposes, we are only interested in the value of the field \vec{E}_R at the dipole's position $\rho = 0$, $z = 0$ (back reaction field). Taking into account the four different reflection possibilities de-

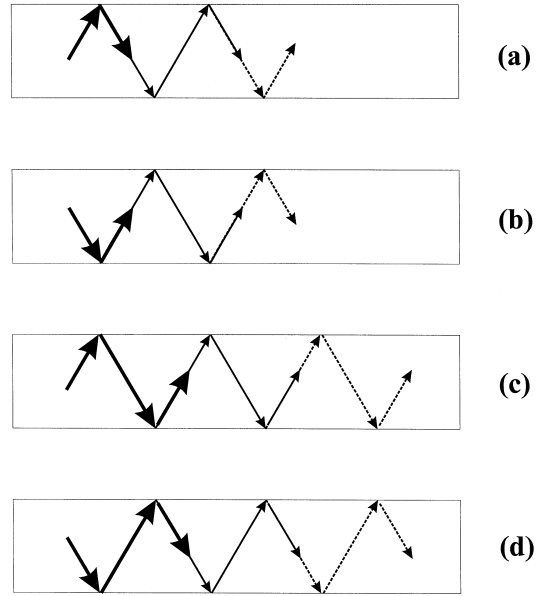


Fig. 3. Schematic illustration of the four distinct cases of plane-wave multiple reflection that give rise to the four integrals in Eq. (9). For further explanation see text.

scribed above, this back reaction field $\vec{E}_R(0)$ is built up by the following four integrals:

$$\vec{E}_R(0) = \frac{ik_0^2}{2\pi} \int \frac{d^2\vec{q}}{l_w} \left(\hat{\kappa}_{pw}^- R_p^1(\hat{\kappa}_{pw}^+ \cdot \vec{p}) + \hat{\kappa}_s R_s^1(\hat{\kappa}_s \cdot \vec{p}) \right) \exp(2idl_w) + \frac{ik_0^2}{2\pi}$$

$$\times \int \frac{d^2\vec{q}}{l_w} \left(\hat{\kappa}_{pw}^+ R_p^0(\hat{\kappa}_{pw}^- \cdot \vec{p}) + \hat{\kappa}_s R_s^0(\hat{\kappa}_s \cdot \vec{p}) \right)$$

$$+ \frac{ik_0^2}{2\pi} \int \frac{d^2\vec{q}}{l_w} \left(\hat{\kappa}_{pw}^+ R_p^0 r_p^1(\hat{\kappa}_{pw}^+ \cdot \vec{p}) + \hat{\kappa}_s R_s^0 r_s^1(\hat{\kappa}_s \cdot \vec{p}) \right) \exp(2idl_w)$$

$$+ \frac{ik_0^2}{2\pi} \int \frac{d^2\vec{q}}{l_w} \left(\hat{\kappa}_{pw}^- R_p^1 r_p^0(\hat{\kappa}_{pw}^- \cdot \vec{p}) + \hat{\kappa}_s R_s^1 r_s^0(\hat{\kappa}_s \cdot \vec{p}) \right) \exp(2idl_w). \quad (9)$$

where the $R_{p,s}^{0,1}$ are multiple reflection coefficients given by

$$R_{p,s}^{0,1}(l_w) = \frac{r_{p,s}^{0,1}(l_w)}{1 - r_{p,s}^0(l_w)r_{p,s}^1(l_w)\exp(2ihl_w)}. \quad (10)$$

It remains to determine which part of the dipole emission is radiated into the glass. Thus, we need to know the transmission coefficients $t_{p,s}$ for a plane p - and s -wave at the spacer/glass interface. These are again given by Fresnel's formulas:

$$t_p(l_w) = \frac{2n_w n_{gl} l_w}{n_{gl}^2 l_w + n_w^2 l_{gl}}, \quad t_s(l_w) = \frac{2l_w}{l_w + l_{gl}}. \quad (11)$$

Considering the transitions of the plane waves in representation Eq. (6) into the glass, and taking into account all multiple reflection possibilities, two qualitatively different processes have to be distinguished: transitions of plane waves with an even number of reflections within the spacer layer (Fig. 4a), and transitions with an uneven number of reflections (Fig. 4b). Then, the transmitted electric field on the glass side is given by

$$\begin{aligned} \vec{E}_T(\vec{r}) &= \frac{ik_0^2}{2\pi} \int \frac{d^2\vec{q}}{l_w} \\ &\times \left(\hat{\kappa}_{p_{gl}}^- t_p \frac{R_p^0}{r_p^0} (\hat{\kappa}_{p_w}^- \cdot \vec{p}) + \hat{\kappa}_s t_s \frac{R_s^0}{r_s^0} (\hat{\kappa}_s \cdot \vec{p}) \right) \\ &\times \exp(i\vec{q} \cdot \vec{p} + il_{gl}|z|) + \frac{ik_0^2}{2\pi} \int \frac{d^2\vec{q}}{l_w} \\ &\times \left(\hat{\kappa}_{p_{gl}}^- t_p R_p^1 (\hat{\kappa}_{p_w}^+ \cdot \vec{p}) + \hat{\kappa}_s t_s R_s^1 (\hat{\kappa}_s \cdot \vec{p}) \right) \\ &\times \exp(i\vec{q} \cdot \vec{p} + il_{gl}|z| + 2idl_w) \end{aligned} \quad (12)$$

where the additional unit vector

$$\hat{\kappa}_{p_{gl}}^- = \frac{1}{k_{gl}} (l_{gl} \hat{q}, q) \quad (13)$$

was introduced.

The flux intensity \vec{S} of electromagnetic radiation is given by the Poynting vector \vec{S} :

$$\vec{S} = \frac{c}{8\pi} \text{Re}(\vec{E}^* \times \vec{B}). \quad (14)$$

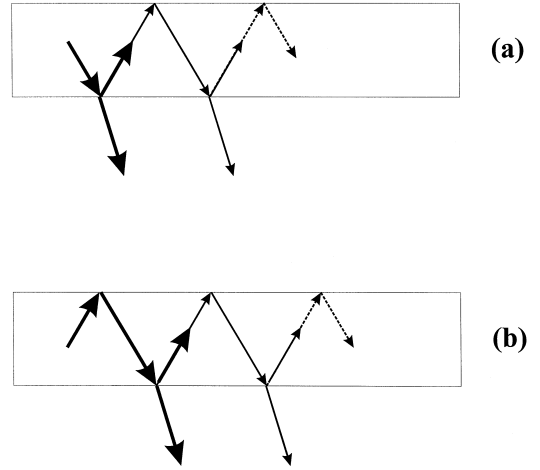


Fig. 4. Schematic illustration of the two distinct cases of plane-wave multiple reflection and transmission that give rise to the two integrals in Eq. (12). For further explanation see text.

For a propagating plane wave, $\vec{E} \exp(i\vec{k}_{gl} \cdot \vec{r})$, the flux intensity of electromagnetic radiation into the direction of \vec{k}_{gl} is given by $S = (cn_{gl}/8\pi) |\vec{E}|^2$. By comparing this with the plane wave representation of \vec{E}_T in Eq. (12), one finds that the flux intensity emitted into the glass half-space ($z < 0$) into a solid angle element $d\Omega_{gl}^2$ in direction $\vec{k}_{gl} = (\vec{q}, -l_{gl})$ will be proportional to [23]

$$\begin{aligned} \frac{d^2S}{d\Omega_{gl}^2} &= C \left| \frac{k_0^2 l_{gl} n_{gl}}{2\pi l_w} \right|^2 \cdot \left[\hat{\kappa}_{p_{gl}}^- t_p \frac{R_p^0}{r_p^0} \hat{\kappa}_{p_w}^- + \hat{\kappa}_s t_s \frac{R_s^0}{r_s^0} \hat{\kappa}_s \right. \\ &\quad \left. + \left(\hat{\kappa}_{p_{gl}}^- t_p R_p^1 \hat{\kappa}_{p_w}^+ + \hat{\kappa}_s t_s R_s^1 \hat{\kappa}_s \right) e^{2idl_w} \right] \cdot \vec{p}^2 \end{aligned} \quad (15)$$

Here, C denotes a proportionality constant. In deriving Eq. (15) we have taken into account that the solid angle element $d\Omega_{gl}^2$ is given by

$$d\Omega_{gl}^2 = \frac{d^2\vec{q}}{k_0 n_{gl} l_{gl}}. \quad (16)$$

The constant C can be found by noting that Eq. (15) has to describe the angular distribution of radiation of a free dipole, $(ck_0^2/8\pi n_{gl}) (k_{gl}^2 p^2 - (\vec{k}_{gl} \cdot \vec{p})^2)$, in the case of equal refractive indices for all layers,

$n_w = n_m = n_{gl}$. Then, $R_p^1 = R_s^1 = 0$, $t_p = t_s = 1$, $R_{p,s}^0/r_{p,s}^0 \rightarrow 1$, and one obtains

$$C = \frac{\pi c}{2n_{gl}^2 k_0^2}. \tag{17}$$

For finding the total emission S_- which is collected by an (loss-free) immersion-oil microscope objective with numerical aperture NA, one has to integrate Eq. (15) of the solid angle of collection of the objective. Thus,

$$S_- = \int_0^{\theta_{max}} d\theta \int_0^{2\pi} d\phi \frac{d^2 S}{d\Omega_{gl}^2} \tag{18}$$

where $\theta_{max} = \arcsin(NA/n_{gl})$, $\theta = \arctan(|\vec{q}|/l_{gl})$, and $\phi = \arctan(q_y/q_x)$.

With the results of Eq. (1), Eq. (9), Eq. (15), and Eq. (18), we are able to compute the average number of photons that are emitted by a molecule and collected by the microscope objective. Assuming that photodestruction occurs only when the molecule is in the excited state, the photodestruction yield will be proportional to the lifetime of the excited state, which is given by $\tau = S_0\tau_0/S$, where τ_0 denotes the lifetime of the free dipole. On the other hand, the quantity of photons emitted into the glass is given by S_-/S . Now, the average number N of photons which is emitted into the objective until the molecule is photobleached is proportional to the product of S_-/S and the inverse of the photobleaching yield. Thus, we arrive at

$$N = S_-N_0/S_0 \tag{19}$$

where N_0 is the average number of photons emitted by a free molecule until photobleaching.

The interesting result is that although the ratio S_-/S may be quite small (only a very small part of the molecule's energy is emitted into the glass), the number N can be reasonably large. In other words, although for every excitation–emission cycle the probability to detect a photon is small, this is compensated for by the much reduced lifetime of the excited state causing the molecule to survive many more excitation–emission cycles than without quenching.

3. Numerical results and discussion

In the numerical calculations, we have chosen the following parameter values: $n_w = 1.33$, $n_{gl} = 1.5$, emission wavelength $\lambda = 670$ nm (emission maximum of the common Cy5 dye). We performed calculations for films of the following metals: silver, gold, copper, aluminum, beryllium, chrome, nickel, palladium, platinum, titanium and tungsten. For calculating the corresponding complex refractive indices, we used a Brendel–Bormann model as described in [24]. It transpired that for the chosen emission wavelength aluminum had the most dramatic effect on the emission properties. Here, we will only show results for aluminum and silver films. The result for gold is nearly identical to that for silver. At 670 nm, the complex refractive index of aluminum is $n_m = 1.45 + 7.7i$, and for silver it is $n_m = 0.16 + 4.07i$. As a

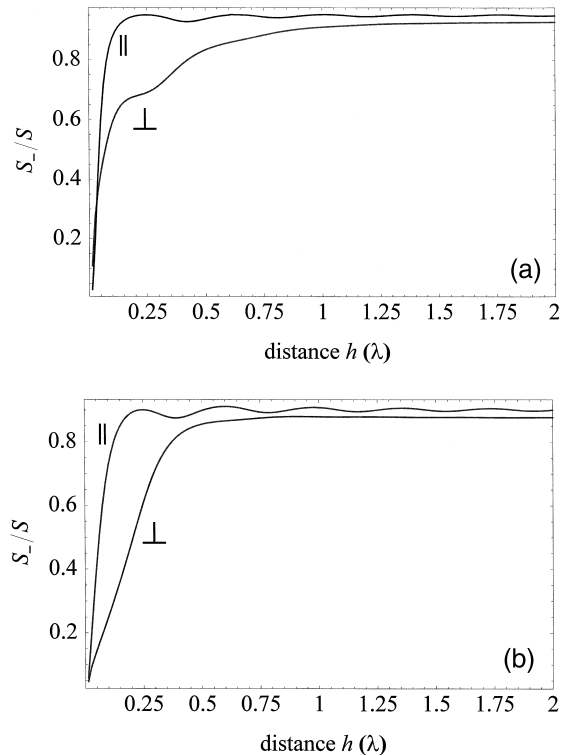


Fig. 5. (a) Ratio S_-/S of the emission rate into the microscope objective S_- to the total de-excitation rate S versus distance h from a 20 nm aluminum film for vertical (\perp) and parallel (\parallel) emission dipole orientation. The distance h is given in units of the wavelength λ . (b) Same as Fig. 5a, but for a 20 nm silver film.

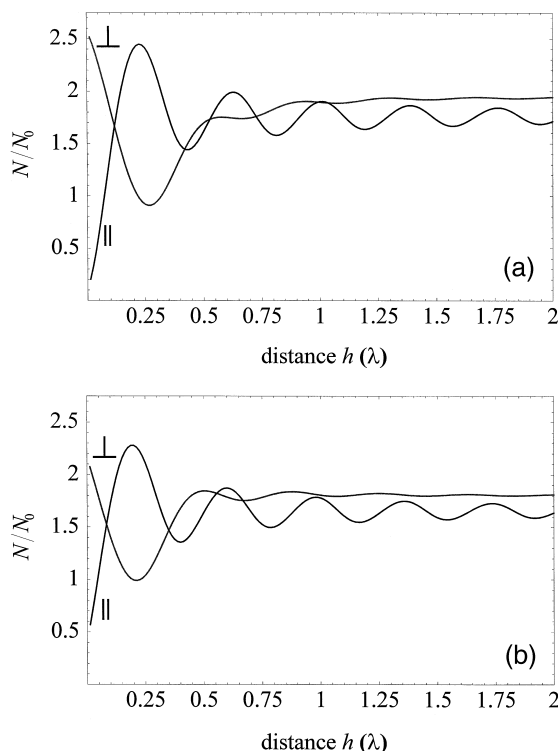


Fig. 6. (a) Ratio $N/N_0 = S_-/S_0$ of the number of detectable photons for the glass/spacer/aluminum film (20 nm) system to that in the homogeneous case ($n_w = 1.33$). Shown are the results for vertical (\perp) and parallel (\parallel) emission dipole orientation. The distance h is given in units of the wavelength λ . (b) Same as Fig. 6a, but for a 20 nm silver film.

typical value for film thickness we have chosen $d = 20$ nm, and the numerical aperture NA of the microscope objective was assumed to be 1.4.

In Fig. 5, the ratio S_-/S of the emission rate into the objective, S_- , to the total de-excitation rate, S , was plotted against the film distance, h , for vertical (along z -direction) and parallel (with respect to the interface) emission dipole orientations. As can be seen, for small values of h , one has strong fluorescence quenching resulting in a very low probability to detect a photon from the excited molecule. But the situation changes if one plots the ratio $N/N_0 = S_-/S_0$, as shown in Fig. 6. This ratio gives the average number of detected photons compared with that emitted into a solid angle of 2π by a free dye molecule in a medium with refractive index n_w . For a vertical dipole orientation and direct adjacency of the metal film ($h = 0$), the average number of de-

tectable photons is more than two times larger than N_0 . But even for a parallel dipole orientation, the average number of detectable photons is much higher than one would expect from looking at Fig. 5. The ratio N/N_0 is larger than unity for large values of h because of the fact that the metal film is reflecting light back into the glass and also that the jump in the refractive index from n_w to n_{gl} at the molecule's position favors emission into the glass.

In our considerations, we did not pay any attention to light scattering. For detecting all the possible photons from a molecule near a metal film until photobleaching, one has to excite it much more often than is the case for a molecule without metal film. A possible approach would be fluorescence excitation by surface-plasmon excitation within the metal film, as indicated in Fig. 1. Surface plasmons yield a high but localized field strength in the direct vicinity of the metal film, thus being a good means for fluorescence excitation without causing too much scattering. Indeed, such an approach was used by Yokota et al. [19] in their successful detection of single molecules on metal films. In their work, they noticed that silver films yield a roughly five-times higher fluorescence intensity than aluminum films. This discrepancy to our result is probably caused by the much better efficiency of surface-plasmon excitation in silver films than in aluminum films. In the present paper, we were concerned only with the properties of fluorescence emission, but did not take into account particularities of the fluorescence excitation.

Acknowledgements

I thank Martin Böhmer (Regensburg University) for many enlightening discussions. I am grateful to Richard Ansell (Regensburg University) for his linguistic support.

References

- [1] K.H. Drexhage, in: E. Wolf (Ed.), *Progress in Optics XII*, North-Holland, Amsterdam, 1974, p. 165.
- [2] R.R. Chance, A. Prock, R. Silbey, in: I. Prigogine, S.R. Rice (Eds.), *Advances in Chemical Physics*, Wiley, New York, 1978, p. 1.

- [3] W. Lukosz, R.E. Kunz, *Opt. Commun.* 20 (1977) 195.
- [4] W. Lukosz, R.E. Kunz, *JOSA* 67 (1977) 1607.
- [5] W. Lukosz, *JOSA* 69 (1979) 1495.
- [6] W. Lukosz, *JOSA* 71 (1981) 744.
- [7] W. Lukosz, R.E. Kunz, *JOSA* 67 (1977) 1615.
- [8] W. Lukosz, *Phys. Rev. B* 15 (1980) 3030.
- [9] M. Lieberherr, C. Fattinger, W. Lukosz, *Surf. Sci.* 189/190 (1987) 954.
- [10] M. Lieberherr, Dissertation, ETH Zürich, 1991.
- [11] W.P. Ambrose, P.M. Goodwin, J.C. Martin, R.A. Keller, *Phys. Rev. Lett.* 72 (1994) 160.
- [12] X.S. Xie, R.C. Dunn, *Science* 265 (1994) 361.
- [13] T. Ha, Th. Enderle, D.S. Chemla, P.R. Selvin, S. Weiss, *Phys. Rev. Lett.* 77 (1996) 3979.
- [14] T. Ha, T. Enderle, D.S. Chemla, P.R. Selvin, S. Weiss, *Chem. Phys. Lett.* 271 (1997) 1.
- [15] R.M. Dickson, A.B. Cubitt, R.Y. Tsien, W.E. Moerner, *Nature* 388 (1997) 355.
- [16] T. Ha, J. Glass, T. Enderle, D.S. Chemla, S. Weiss, *Phys. Rev. Lett.* 80 (1998) 2093.
- [17] K.D. Weston, S.K. Buratto, *J. Phys. Chem. A* 102 (1998) 3635.
- [18] K.D. Weston, P.J. Carson, H. Metiu, S.K. Buratto, *J. Chem. Phys.* 109 (1998) 7474.
- [19] H. Yokota, K. Saito, T. Yanagida, *Phys. Rev. Lett.* 80 (1998) 4606.
- [20] T. Hirschfeld, *Appl. Opt.* 15 (1976) 3135.
- [21] S.D. Brorson, in: H. Yokoyama, K. Ujihara (Eds.), *Spontaneous Emission and Laser Oscillations in Microcavities*, CRC Press, Boca Raton, 1995, p. 151.
- [22] J.D. Jackson, *Classical Electrodynamics*, Wiley, New York, 1975, p. 278.
- [23] J. Enderlein, T. Ruckstuhl, S. Seeger, *Appl. Opt.* 38 (1999) 724.
- [24] A.D. Rakic, A.B. Djuricic, J.M. Elazar, M.L. Majewski, *Appl. Opt.* 37 (1998) 5271.